Fictitious time wave packet dynamics: The hydrogen atom in external fields

Tomaž Fabčič, Jörg Main, and Günter Wunner

Institut für Theoretische Physik 1, Universität Stuttgart, 70550 Stuttgart, Germany

(Dated: October 2, 2008)

In the preceding paper [T. Fabčič et al., preprint] "restricted Gaussian wave packets" were introduced for the regularized Coulomb problem in the four-dimensional Kustaanheimo-Stiefel coordinates, and their exact time propagation was derived analytically in a fictitious time variable. We now establish the Gaussian wave packet method for the hydrogen atom in static external fields. A superposition of restricted Gaussian wave packets is used as a trial function in the application of the time-dependent variational principle. The external fields introduce couplings between the basis states. The set of coupled wave packets is propagated numerically, and eigenvalues of the Schrödinger equation are obtained by the frequency analysis of the time autocorrelation function. The advantage of the wave packet propagation in the fictitious time variable is that the computations are exact for the field-free hydrogen atom and approximations from the time-dependent variational principle only stem from the external fields. Examples are presented for the hydrogen atom in a magnetic field and in crossed electric and magnetic fields.

I. INTRODUCTION

The hydrogen atom in a static magnetic field [1–5] and in crossed electric and magnetic fields [6–16] is a nonintegrable system which can be accessed both experimentally and theoretically and has attracted much attention during recent decades. Exact quantum spectra of the system can be obtained by numerical diagonalization of the Hamiltonian in a large Sturmian type basis set. Nevertheless, the atom has served as an example system for the development and verification of alternative quantization methods, e.g., semiclassical closed-orbit theory [17, 18], periodic-orbit theory [19, 20], and cycle-expansion techniques [21].

Another alternative to large quantum computations is the application of the time-dependent variational principle (TDVP) [22]. For a wave packet depending on a set of variational parameters the time-dependent Schrödinger equation is transformed to a system of ordinary differential equations for the variational parameters. Quantum spectra can be obtained by a frequency analysis of the time autocorrelation function of the wave packet. The method has been established by Heller [23, 24] for single or coupled Gaussian wave packets (GWPs). It is well suited for nonsingular smooth potentials but certainly far from ideal for atomic systems with singular Coulomb potentials.

The wave packet dynamics in atomic systems has been studied for the field-free hydrogen atom [25–27], and in particular for the atom in time-dependent external fields, e.g., microwaves or short laser pulses. While Rydberg wave packets are usually dispersive, the possible existence of nondispersive coherent states has been demonstrated for the hydrogen atom in microwave fields [28, 29].

In the preceding paper [30] we have established the Gaussian wave packet method for the Coulomb problem. Using the Kustaanheimo-Stiefel (KS) regularization the singular Coulomb problem was transformed to the four-dimensional (4D) harmonic oscillator with a constraint. We introduced the set of "restricted Gaussian wave packets" obeying that constraint by confining the space of the Gaussian parameters. The exact propagation of the restricted GWPs in a fictitious time variable could be derived analytically.

In this paper we extend the fictitious time wave packet propagation to the hydrogen atom in static external electric and magnetic fields. A superposition of restricted GWPs is used as the variational trial function. The time-dependent variational principle is applied in such a way that the wave packet dynamics is exact for the field-free hydrogen atom and couplings between the GWPs are only induced by the external fields. In the presence of a single external homogeneous field the rotational symmetry of the hydrogen atom is preserved and one component of the angular momentum, say l_z, is conserved. In that case we employ the modified 2D Gaussian wave packets with well-defined magnetic quantum number m introduced and discussed in Ref. [30] and perform computations in the subspaces of the different magnetic quantum numbers m separately. In crossed fields the cylindrical symmetry is broken and computations are performed in the basis of the restricted 3D GWPs without well-defined angular momentum quantum numbers.

The paper is organized as follows. In Sec. II we introduce the regularization and scaling of the Hamiltonian with external fields and discuss the general idea of how to obtain quantum spectra by frequency analysis of the fictitious time autocorrelation function of the propagated wave packets. In Sec. III the time-dependent variational principle is explained. The equations of motion for the variational parameters are derived for the superposition of restricted 3D and modified 2D GWPs, and the numerical time propagation of coupled wave packets is discussed. Results for the diamagnetic hydrogen atom and the atom in crossed electric and magnetic fields are presented in Sec. IV. Concluding remarks are given in Sec. V.

II. REGULARIZED HYDROGEN ATOM IN EXTERNAL FIELDS

In the preceding paper [30] the fictitious time wave packet dynamics has been discussed for the field-free hydrogen atom. We now consider the atom in external electric and magnetic fields. For perpendicular fields with the electric and magnetic field along the x and z axis, respectively, the Hamiltonian in the three-dimensional coordinates reads (in atomic units with $F_0 = 5.14 \times 10^9 \mathrm{V/cm}$, $B_0 = 2.35 \times 10^5 \mathrm{T}$)

$$H_3 = \frac{1}{2}\mathbf{p}^2 - \frac{1}{r} + \frac{1}{2}Bl_z + \frac{1}{8}B^2(x^2+y^2) + Fx . \quad (1)$$

The starting point for our investigations is the Schrödinger equation in the 4D Kustaanheimo-Stiefel coordinates $\mathbf{u}$ with $x = u_1u_3 - u_2u_4$, $y = u_1u_4 + u_2u_3$, and $z = \frac{1}{2}(u_1^2 + u_2^2 - u_3^2 - u_4^2)$. Introducing scaled coordinates and momenta $\mathbf{u} \to n_{\mathrm{eff}}^{1/2}\mathbf{u}$, $\mathbf{p}_u \to n_{\mathrm{eff}}^{-1/2}\mathbf{p}_u$ and following the procedure of Sec. II in [30] we obtain

$$\begin{aligned} H\psi &= \left\{ \frac{1}{2}\mathbf{p}_u^2 + \left[-n_{\mathrm{eff}}^2 E + \frac{1}{8}(n_{\mathrm{eff}}^2 B)^2(u_1^2+u_2^2)(u_3^2+u_4^2) \right.\right. \\ &\quad \left. + n_{\mathrm{eff}}^3 F(u_1u_3 - u_2u_4) \right] \mathbf{u}^2 \\ &\quad + \frac{1}{2}n_{\mathrm{eff}}^2 B \left[(u_1p_2 - u_2p_1)(u_3^2+u_4^2) \right. \\ &\quad \left.\left. + (u_3p_4 - u_4p_3)(u_1^2+u_2^2) \right] \right\} \psi = 2n_{\mathrm{eff}}\,\psi . \end{aligned} \quad (2)$$

In KS coordinates physical wave functions must fulfill the constraint

$$(u_2p_1 - u_1p_2 - u_4p_3 + u_3p_4)\,\psi = 0 . \quad (3)$$

By choosing constant parameters

$$\alpha \equiv -n_{\mathrm{eff}}^2 E , \quad \beta \equiv n_{\mathrm{eff}}^2 B , \quad \zeta \equiv n_{\mathrm{eff}}^3 F , \quad (4)$$

Eq. (2) becomes an eigenvalue problem for the effective quantum number n_{eff}. For a set of parameters (α, β, ζ) and a given eigenvalue n_{eff} the energy and field strengths of the physical state are obtained from Eq. (4). The quantized energies and field strengths are located on lines with constant E/B and $E/F^{2/3}$.

In analogy with the field-free hydrogen atom in [30] we can extend Eq. (2) to the time-dependent Schrödinger equation in the fictitious time τ by the replacement $2n_{\mathrm{eff}} \to i\frac{\partial}{\partial\tau}$, viz.

$$i\frac{\partial}{\partial\tau}\psi = \left(\frac{1}{2}\mathbf{p}_u^2 + V \right)\psi = \left(-\frac{1}{2}\Delta_4 + V \right)\psi = (T+V)\psi , \quad (5)$$

where V is defined via Eq. (2) as the sum of a harmonic potential and the contributions of the external fields. For the field-free hydrogen atom, i.e., a harmonic potential V, wave packets can be propagated analytically in the fictitious time [30].

Our goal for the hydrogen atom in external fields is to compute the propagation of an initial wave packet $\psi(0)$ by applying the time-dependent variational principle. To this end the wave function is assumed to depend on a set of appropriately chosen parameters whose time-dependence is obtained by solving ordinary differential equations. The ansatz for the wave function depends on the symmetry of the problem. For the hydrogen atom in crossed fields we choose a superposition of N restricted Gaussian wave packets [30]

$$\psi(\tau) = \sum_{k=1}^{N} e^{i[\mathbf{u}A_k(\tau)\mathbf{u}+\gamma_k(\tau)]} , \quad (6)$$

with the symmetric width matrices

$$A = \begin{pmatrix} a_\mu & 0 & a_x & a_y \\ 0 & a_\mu & a_y & -a_x \\ a_x & a_y & a_\nu & 0 \\ a_y & -a_x & 0 & a_\nu \end{pmatrix} , \quad (7)$$

depending on the four parameters (a_μ, a_ν, a_x, a_y), and with γ determining the normalization and phase of the restricted GWPs. The special form of the ansatz (6), which depends on, in total, $5N$ time-dependent variational parameters (instead of $15N$ complex parameters for the most general superposition of Gaussian wave packets in a 4D coordinate space) guarantees that the wave function obeys the constraint (3).

The hydrogen atom in a pure magnetic field, i.e., $\zeta = 0$, is cylindrically symmetric around the z axis, and the angular momentum component $l_z = m$ is an exact quantum number. For wave packets with given m quantum number we use the ansatz

$$\begin{aligned} \psi_m(\tau) &= (\mu\nu)^{|m|} \sum_{k=1}^{N} e^{i[\mathbf{u}A_k(\tau)\mathbf{u}+\gamma_k(\tau)]}e^{im\varphi} \\ &= (\mu\nu)^{|m|} \sum_{k=1}^{N} e^{i[a_\mu^k(\tau)\mu^2 + a_\nu^k(\tau)\nu^2 + \gamma_k(\tau)]}e^{im\varphi}, \end{aligned} \quad (8)$$

with the diagonal form of the matrix A obtained by setting $a_x = a_y = 0$ in (7), and semiparabolic coordinates $\mu = \sqrt{u_1^2 + u_2^2} = \sqrt{r+z}$ and $\nu = \sqrt{u_3^2 + u_4^2} = \sqrt{r-z}$ are introduced. The wave function (8) thus depends on a set of $3N$ time-dependent variational parameters. As the paramagnetic term is constant this term can be absorbed by an energy shift $E \to E' = E - mB/2$. In semiparabolic coordinates the kinetic and potential term in (5) for the diamagnetic hydrogen atom then take the form

$$T = -\frac{1}{2}\left(\frac{\partial^2}{\partial\mu^2} + \frac{1}{\mu}\frac{\partial}{\partial\mu} - \frac{m^2}{\mu^2} + \frac{\partial^2}{\partial\nu^2} + \frac{1}{\nu}\frac{\partial}{\partial\nu} - \frac{m^2}{\nu^2} \right) ,$$

$$V = \alpha(\mu^2 + \nu^2) + \frac{1}{8}\beta^2(\mu^4\nu^2 + \mu^2\nu^4) . \quad (9)$$

Once the time-dependent wave packets (6) or (8) are determined the eigenvalues $n_{\mathrm{eff}}^{(j)}$ of the stationary

Schrödinger equation (2) and thus quantum spectra of the hydrogen atom in external fields are obtained by a frequency analysis of the time signal

$$C(\tau) = \langle\psi(0)|\psi(\tau)\rangle = \sum_j c_j e^{-i2n_{\text{eff}}^{(j)}\tau} , \qquad (10)$$

with the amplitudes c_j depending on the choice of the initial wave packet. The advantage of using the fictitious time τ is that the computations are exact for the field-free hydrogen atom and approximations from the time-dependent variational principle only stem from the external fields. By contrast, wave packet propagation in the physical time t is a very nontrivial task even for the pure Coulomb potential.

III. TIME-DEPENDENT VARIATIONAL PRINCIPLE

The propagation of the wave packets investigated in this paper is based on the application of the time-dependent variational principle. For the convenience of the reader we first give a brief general introduction to the TDVP which is then applied to the special form of the trial functions (6) and (8). The formulation of McLachlan [22], or equivalently the minimum error method [31], requires the norm of the deviation between the right-hand and the left-hand side of the time-dependent Schrödinger equation to be minimized with respect to the trial function. The quantity

$$I = ||i\phi(t) - H\psi(t)||^2 \overset{!}{=} \min \qquad (11)$$

is to be varied with respect to ϕ only, and then $\dot{\psi} \equiv \phi$ is chosen, i.e., for any time t the fixed wave function $\psi(t)$ is supposed to be given and its time derivative $\dot{\psi}(t)$ is determined by the requirement to minimize I. The equality $I = 0$ is provided by the exact solution of the Schrödinger equation, while I in general takes positive values if $\dot{\psi}$ is constrained by the functional form of ψ. The wave function $\psi(t)$ is assumed to be parametrized by a set of complex parameters $\mathbf{z}(t) = (z_1(t), \ldots, z_{n_p}(t))$, $\psi(t) = \psi(\mathbf{z}(t))$. For brevity the arguments of the wave function are dropped in the following. For parametrized trial functions the variations $\delta\phi$ carry over to variations $\delta\dot{\mathbf{z}}$ and the variation leads to the equations of motion

$$\left\langle \frac{\partial\psi}{\partial\mathbf{z}} \Big| i\dot{\psi} - H\psi \right\rangle = 0 , \qquad (12)$$

which can be written in matrix form

$$K\dot{\mathbf{z}} = -i\mathbf{h} \quad \text{with} \quad K = \left\langle \frac{\partial\psi}{\partial\mathbf{z}} \Big| \frac{\partial\psi}{\partial\mathbf{z}} \right\rangle , \quad \mathbf{h} = \left\langle \frac{\partial\psi}{\partial\mathbf{z}} \Big| H\psi \right\rangle . \qquad (13)$$

An illustration of Eq. (12) is presented in Fig. 1. Here the manifold of approximation M, consisting of all possible configurations $\psi(\mathbf{z})$, is plotted schematically as a
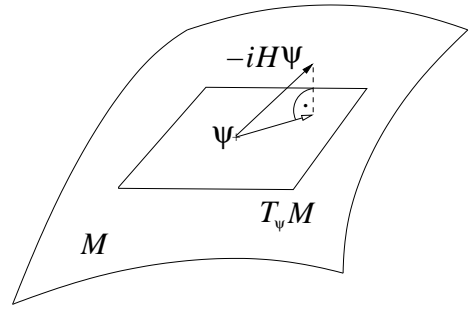

FIG. 1: Sketch of the manifold M of approximation of the trial wave function $\psi(\mathbf{z})$. The variational evolution of the trial function, denoted by the arrow with the white arrowhead, is obtained as the projection of the exact time evolution $-iH\psi$, denoted by the arrow with the black arrowhead, onto the tangent space $T_\psi M$ of the manifold M in the point ψ.

2D-surface in the Hilbert space. The tangent space of the manifold in the point ψ is a linear vector space and is spanned by the derivatives $\frac{\partial\psi}{\partial z_k}$, $k = 1, \ldots, n_p$. The tangent space is denoted by $T_\psi M$ in Fig. 1. According to the Schrödinger equation the exact time derivative $\dot{\psi}$ is given by $-iH\psi$, denoted by the arrow with the black arrowhead. In general the exact time derivative does not lie in the tangent space, otherwise the trial function would be an exact solution of the Schrödinger equation. The variational approximation to the exact time derivative is given by that vector of the tangent space which has minimal deviation from the exact one. This is the orthogonal projection of the exact time derivative onto the tangent space, denoted by the arrow with the white arrowhead in Fig. 1.

For parametrized wave functions the variational principle (11) simply reduces to a quadratic minimization problem where the gradient of I with respect to the time derivatives of the parameters must be zero

$$\frac{\partial I}{\partial\dot{z}_k} = 0 , \quad k = 1, \ldots, n_p , \qquad (14)$$

and the TDVP leads to a reduction of the Schrödinger equation to a system of ordinary first-order differential equations of motion for the parameters $\mathbf{z}(t)$. The matrix equation (13) must be solved numerically after each time step of integration for the time derivatives $\dot{\mathbf{z}}$ if a numerical algorithm for ordinary differential equations, e.g. Runge-Kutta or Adams, is used.

We now apply the time-dependent variational principle, first in Sec. III A to the trial function (8) of the diamagnetic hydrogen atom, and then in Sec. III B to the trial function (6) of the hydrogen atom in crossed electric and magnetic fields. For Gaussian type trial functions it is convenient to split the Hamiltonian into the kinetic and potential part, i.e., $H = T + V$, and to apply Eq. (12) in the form

$$\left\langle \frac{\partial\psi}{\partial\mathbf{z}} \Big| i\dot{\psi} - T\psi \right\rangle = \left\langle \frac{\partial\psi}{\partial\mathbf{z}} \Big| V\psi \right\rangle . \qquad (15)$$

A. Diamagnetic hydrogen atom

For the time-dependent wave packets of the hydrogen atom in a homogeneous external magnetic field with given m quantum number we use the ansatz (8) which can be written in the form

$$\psi_m = \psi_m(\mathbf{z}) = \sum_{k=1}^{N} g_m(\mathbf{y}^k) \,, \qquad (16)$$

with the basis states

$$g_m(\mathbf{y}) = (\mu\nu)^{|m|} e^{i(a_\mu \mu^2 + a_\nu \nu^2 + \gamma)} \,. \qquad (17)$$

As already mentioned, the cylindrical symmetry of the system is accounted for by setting $a_x = a_y = 0$ and only the time-dependent parameters $\mathbf{z} = (\mathbf{y}^1, \ldots, \mathbf{y}^N)$ with $\mathbf{y} = (\gamma, a_\mu, a_\nu)$ remain. The evolution of the basis states is obtained by the TDVP. The variational equations of motion are set up by evaluating Eq. (15). First we let the time derivative and the Laplacian act on the basis states (17) to obtain

$$\left(i \frac{\partial}{\partial \tau} - T \right) g_m(\mathbf{y}^k, \mathbf{x})$$
$$= \left[-\dot{\gamma}^k + 2i \left(a_\mu^k + a_\nu^k \right) (1 + |m|) - (\dot{a}_\mu^k + 2(a_\mu^k)^2)\mu^2 - (\dot{a}_\nu^k + 2(a_\nu^k)^2)\nu^2 \right] g_m(\mathbf{y}^k, \mathbf{x})$$
$$\equiv \left[v_0^k + \frac{1}{2} \left(V_\mu^k \mu^2 + V_\nu^k \nu^2 \right) \right] g_m(\mathbf{y}^k, \mathbf{x}) \,, \qquad (18)$$

for $k = 1, \ldots, N$. Eq. (18) defines the coefficients v_0^k, V_μ^k, V_ν^k as functions of the parameters a_μ^k, a_ν^k and the time derivatives $\dot{\gamma}^k$, $\dot{a}_\mu^k$, $\dot{a}_\nu^k$. The equations of motion can be written as

$$\dot{a}_\mu^k = -2(a_\mu^k)^2 - \frac{1}{2} V_\mu^k \,, \qquad (19a)$$

$$\dot{a}_\nu^k = -2(a_\nu^k)^2 - \frac{1}{2} V_\nu^k \,, \qquad (19b)$$

$$\dot{\gamma}^k = 2i \left(a_\mu^k + a_\nu^k \right) (1 + |m|) - v_0^k \,, \qquad (19c)$$

with $k = 1, \ldots, N$, and the yet unknown coefficients V_μ^k, V_ν^k, and v_0^k. Note that the equations of motion (19) are in general coupled through the coefficients v_0^k, V_μ^k, V_ν^k which become time-dependent in the presence of anharmonic potentials. They must be determined from a system of linear equations, which follows from Eq. (15) when inserting the trial function (16). Using the derivatives of the basis states (17) with respect to the variational parameters, viz. $\frac{\partial}{\partial \gamma^k} g_m^k = i g_m^k$, $\frac{\partial}{\partial a_\mu^k} g_m^k = i\mu^2 g_m^k$, and $\frac{\partial}{\partial a_\nu^k} g_m^k = i\nu^2 g_m^k$, Eq. (15) of the TDVP finally yields the matrix equation

$$\sum_{k=1}^{N} \left(\langle g_m^l | g_m^k \rangle v_0^k + \frac{1}{2} \langle g_m^l | \mu^2 | g_m^k \rangle V_\mu^k + \frac{1}{2} \langle g_m^l | \nu^2 | g_m^k \rangle V_\nu^k \right) = \sum_{k=1}^{N} \langle g_m^l | V(\mu, \nu) | g_m^k \rangle \,,$$

$$\sum_{k=1}^{N} \left(\langle g_m^l | \mu^2 | g_m^k \rangle v_0^k + \frac{1}{2} \langle g_m^l | \mu^4 | g_m^k \rangle V_\mu^k + \frac{1}{2} \langle g_m^l | \mu^2 \nu^2 | g_m^k \rangle V_\nu^k \right) = \sum_{k=1}^{N} \langle g_m^l | \mu^2 V(\mu, \nu) | g_m^k \rangle \,,$$

$$\sum_{k=1}^{N} \left(\langle g_m^l | \nu^2 | g_m^k \rangle v_0^k + \frac{1}{2} \langle g_m^l | \mu^2 \nu^2 | g_m^k \rangle V_\mu^k + \frac{1}{2} \langle g_m^l | \nu^4 | g_m^k \rangle V_\nu^k \right) = \sum_{k=1}^{N} \langle g_m^l | \nu^2 V(\mu, \nu) | g_m^k \rangle \,, \qquad (20)$$

where the index $l = 1, \ldots, N$ runs over all basis states and the notation $g_m^k \equiv g_m(\mathbf{y}^k)$ is used. The potential $V(\mu, \nu)$ for the diamagnetic hydrogen atom is given in Eq. (9). All integrals in Eq. (20) can be obtained analytically, and are presented in Appendix A. The set of equations (20) is a $3N$-dimensional Hermitian positive semidefinite linear system for the coefficients v_0^k, V_μ^k, V_ν^k, $k = 1, \ldots, N$, and must be solved, e.g., using a Cholesky decomposition [32] of the left-hand side matrix, at every time step when numerically integrating the equations of motion (19). Technical remarks for the time propagation of coupled wave packets via the numerical integration of the Eqs. (19) will be given in Sec. III C.

B. Hydrogen atom in crossed fields

The rotational symmetry of the hydrogen atom in a magnetic field as discussed in Sec. III A is broken when an additional electric field with a different orientation is applied. In crossed fields none of the three degrees of freedom can be separated. The paramagnetic term that contributed only a constant energy shift within the subspace of constant m in the diamagnetic hydrogen atom must now be taken into account since l_z is not conserved. The evolution of wave packets is determined by the time-dependent Schrödinger equation (5) with

T given by minus one half times the Laplacian in the 4D Kustaanheimo-Stiefel coordinates, and V defined via Eqs. (2) and (4) as

$$V = \alpha\mathbf{u}^2 + \frac{1}{2}\beta[(u_1p_2 - u_2p_1)(u_3^2 + u_4^2)$$
$$+(u_3p_4 - u_4p_3)(u_1^2 + u_2^2)] \qquad (21)$$
$$+ \frac{1}{8}\beta^2(u_1^2 + u_2^2)(u_3^2 + u_4^2)\mathbf{u}^2 + \zeta(u_1u_3 - u_2u_4)\mathbf{u}^2 .$$

As trial functions for the time-dependent variational principle we use the superposition

$$\psi(\mathbf{z}) = \sum_{k=1}^{N} g(\mathbf{y}^k) \qquad (22)$$

where

$$g^k \equiv g(\mathbf{y}^k) = e^{i(\mathbf{u}A^k\mathbf{u}+\gamma^k)} \qquad (23)$$

are the restricted Gaussian wave packets derived in the preceding paper [30], which depend on the $5N$ time-dependent variational parameters $\mathbf{y}^k = (\gamma^k, a_\mu^k, a_\nu^k, a_x^k, a_y^k)$ (see Eq. (7)), combined in the parameter vector $\mathbf{z} = (\mathbf{y}^1, \ldots, \mathbf{y}^N)$. The equations of motion for the variational parameters are obtained by evaluating the TDVP in Eq. (15) for the trial function (22). The procedure is similar to that in Sec. III A. Letting the time derivative and the Laplacian act on a restricted GWP (23) yields

$$\left(i\frac{\partial}{\partial\tau} - T\right)g^k = \left(-\mathbf{u}\dot{A}^k\mathbf{u} - \dot{\gamma}^k - 2\mathbf{u}(A^k)^2\mathbf{u}\right.$$
$$\left. +i\operatorname{tr}A^k\right)g^k$$
$$\equiv \left(v_0^k + \frac{1}{2}\mathbf{u}V_2^k\mathbf{u}\right)g^k , \qquad (24)$$

and defines a scalar v_0^k and a 4×4 matrix V_2^k as the coefficients of the polynomial in $\mathbf{u}$ for each GWP with $k = 1, \ldots, N$, i.e., $v_0^k = i\operatorname{tr}A^k - \dot{\gamma}^k$ and $V_2^k/2 = -\dot{A}^k - 2(A^k)^2$. Since the special structure of the matrices A^k in Eq. (7) is maintained in the squared matrices $(A^k)^2$, that structure carries over to the 4×4 complex symmetric matrices V_2^k due to their definition in Eq. (24). Therefore, they have only four independent coefficients V_μ^k, V_ν^k, V_x^k, and V_y^k in the notation of Eq. (7). The equations of motion for the variational parameters $\mathbf{y}^k = (\gamma^k, a_\mu^k, a_\nu^k, a_x^k, a_y^k)$, $k = 1, \ldots, N$ can be written as

$$\dot{A}^k = -2(A^k)^2 - \frac{1}{2}V_2^k , \qquad (25a)$$
$$\dot{\gamma}^k = i\operatorname{tr}A^k - v_0^k , \qquad (25b)$$

where the time-dependent parameters $(v_0^k, V_\mu^k, V_\nu^k, V_x^k, V_y^k)$ are obtained at every time step by solving a linear set of equations. Using the derivatives of the restricted GWPs with respect to the variational parameters,

$$\frac{\partial g^k}{\partial\gamma^k} = ig^k , \quad \frac{\partial g^k}{\partial a_\mu^k} = i(u_1^2 + u_2^2)g^k ,$$
$$\frac{\partial g^k}{\partial a_\nu^k} = i(u_3^2 + u_4^2)g^k , \quad \frac{\partial g^k}{\partial a_x^k} = 2i(u_1u_3 - u_2u_4)g^k ,$$
$$\frac{\partial g^k}{\partial a_y^k} = 2i(u_1u_4 + u_2u_3)g^k , \qquad (26)$$

the required linear set of equations is derived from (15) as

$$\sum_{k=1}^{N}\left(I_{11}^{lk}v_0^k + I_{12}^{lk}\frac{1}{2}V_\mu^k + I_{13}^{lk}\frac{1}{2}V_\nu^k + I_{14}^{lk}V_x^k + I_{15}^{lk}V_y^k\right) = \sum_{k=1}^{N}I_{v1}^{lk} ,$$

$$\sum_{k=1}^{N}\left(I_{12}^{lk}v_0^k + I_{22}^{lk}\frac{1}{2}V_\mu^k + I_{23}^{lk}\frac{1}{2}V_\nu^k + I_{24}^{lk}V_x^k + I_{25}^{lk}V_y^k\right) = \sum_{k=1}^{N}I_{v2}^{lk} ,$$

$$\sum_{k=1}^{N}\left(I_{13}^{lk}v_0^k + I_{23}^{lk}\frac{1}{2}V_\mu^k + I_{33}^{lk}\frac{1}{2}V_\nu^k + I_{34}^{lk}V_x^k + I_{35}^{lk}V_y^k\right) = \sum_{k=1}^{N}I_{v3}^{lk} ,$$

$$\sum_{k=1}^{N}\left(I_{14}^{lk}v_0^k + I_{24}^{lk}\frac{1}{2}V_\mu^k + I_{34}^{lk}\frac{1}{2}V_\nu^k + I_{44}^{lk}V_x^k + I_{45}^{lk}V_y^k\right) = \sum_{k=1}^{N}I_{v4}^{lk} ,$$

$$\sum_{k=1}^{N}\left(I_{15}^{lk}v_0^k + I_{25}^{lk}\frac{1}{2}V_\mu^k + I_{35}^{lk}\frac{1}{2}V_\nu^k + I_{45}^{lk}V_x^k + I_{55}^{lk}V_y^k\right) = \sum_{k=1}^{N}I_{v5}^{lk} , \qquad (27)$$

with $l = 1, \ldots, N$. All integrals I in Eq. (27) are defined and listed in Appendix B. The potential (22) for the hydrogen atom in crossed electric and magnetic fields,

including the paramagnetic contribution, enters the integrals on the right-hand side of Eq. (27). The linear set of equations (27) is Hermitian positive semidefinite [see Eq. (20) for the diamagnetic hydrogen atom] and can be solved using a Cholesky decomposition of the left-hand side matrix.

C. Numerical time propagation of coupled wave packets

An initial wave packet given as the superposition of basis states in Eq. (16) or (22) can be easily propagated for the field-free hydrogen atom because the basis states remain uncoupled and the time-dependence of the basis states is known analytically [30]. The external fields lead to couplings between the basis states, and the time-dependence of the variational parameters must be determined numerically. The setup of the equations of motion has been discussed in Secs. III A and III B. The numerical integration, however, of Eqs. (19) and (25) is nontrivial and further remarks are necessary.

1. Time propagation of the width matrices

For better numerical performance it is advantageous [31, 33] to introduce, for each width matrix A, two auxiliary time-dependent 4×4 matrices B and C in such a way that

$$A = \frac{1}{2} B C^{-1} . \tag{28}$$

The equations of motion (25a) and similarly Eqs. (19a) and (19b) are then replaced with the equivalent differential equations

$$\begin{aligned} \dot{B}^k &= -V_2^k C^k , \\ \dot{C}^k &= B^k , \end{aligned} \tag{29}$$

with the initial values $B(0) = 2A(0)$ and $C(0) = \mathbf{1}$. In the case of the diamagnetic hydrogen atom the matrices A and V_2 are diagonal with diagonal elements $\{a_\mu, a_\mu, a_\nu, a_\nu\}$ and $\{V_\mu, V_\mu, V_\nu, V_\nu\}$, respectively. The matrices B and C have the same structure, and thus the total number of parameters per basis state that must be integrated (including the scalar γ) increases from three parameters (γ, a_μ, a_ν) to five parameters $(\gamma, b_\mu, b_\nu, c_\mu, c_\nu)$.

For crossed fields the increase of the number of parameters is even more rapid. In that case the matrices B and C are no more complex symmetric. Without taking care of the special structure (7) of the matrix A the introduction of the B and C matrices would require the integration of 32 complex parameters per GWP in the two matrices B and C instead of four complex parameters in the width matrix A. However, the special structure of the matrix A can be exploited to halve the number of

independent parameters from 32 to 16 in the matrices B and C. Details are given in Appendix C.

When integrating the equations of motion most of the computational effort is invested in solving the set of $3N$ linear equations (20) or the $5N$ linear equations (27) at each time step. The dimension of those equations is not affected by the introduction of the auxiliary matrices B and C, and thus the increase of the number of parameters in the differential equations (29) does not imply a significant increase of the total computing effort. In fact, due to the better numerical behavior of Eq. (29) as compared to Eq. (25a) and Eqs. (19a), (19b), larger step sizes of the numerical integration are possible and the total computing time is decreased.

2. TDVP with constraints

The equations of motion resulting from the TDVP especially for a large number of coupled GWPs become badly behaved from time to time during the integration. In the general formulation of the TDVP at each time step the linear set of equations (13) must be solved for the equations of motion of the variational parameters, i.e., the time derivatives $\dot{\mathbf{z}}$. In the course of integration, depending on the number of coupled GWPs, it will happen sooner or later that the matrix K in Eq. (13) associated with the set of linear equations becomes ill-conditioned, or even numerically singular. As a result the time step of the integration routine becomes extremely small, rendering the method of GWP propagation impracticably slow. In the worst case the wave packet propagation can stick completely.

Matrix singularity problems arise from overcrowding the basis set, i.e., from situations where fewer GWPs would be sufficient to represent the wave function. On the other hand for an accurate approximation of the wave function it is desirable to have a large number of adjustable parameters. However, there is a discrepancy between the number of GWPs necessary to yield accurate results and the maximum number of GWPs that can be propagated using the TDVP without numerical difficulties [34]. There exist different proposals to overcome this numerical problem [31, 34–40]. Here we adopt the constrained time-dependent variational principle [40], where inequality constraints of the form

$$\begin{aligned} f_k(\mathbf{z}, \mathbf{z}^*) &\equiv f_k(\mathbf{z}_r, \mathbf{z}_i) \equiv f_k(\bar{\mathbf{z}}) \geq f_{k,\min} , \\ f_k &\in \mathbb{R}, \ k = 1, 2, 3, \ldots \end{aligned} \tag{30}$$

are taken into account in the variational process, and complex quantities are split into their real and imaginary parts, denoted by the subscripts r and i, respectively, and thus $\bar{\mathbf{z}} \equiv (\mathbf{z}_r, \mathbf{z}_i)$. The functions f_k must be chosen in such a way to prevent the matrix K from becoming singular. As long as $f_k(\mathbf{z}_r, \mathbf{z}_i) > f_{k,\min}$ for all k, all parameters evolve according to Eq. (13) without being affected by the constraints. However, when $f_k(\mathbf{z}_r, \mathbf{z}_i) = f_{k,\min}$

and $\dot{f}_k(\mathbf{z}_r, \mathbf{z}_i) < 0$ for, say, $k = 1, \ldots, j$ we introduce Lagrangian multipliers and obtain an extended set of linear equations

$$\left(\begin{array}{c|c} \bar{K} & \bar{M}^T \\ \hline \bar{M} & 0 \end{array} \right) \left(\begin{array}{c} \dot{\bar{\mathbf{z}}} \\ \boldsymbol{\lambda} \end{array} \right) = \left(\begin{array}{c} \bar{\mathbf{h}} \\ 0 \end{array} \right),$$

$$\text{with } \bar{K} = \left(\begin{array}{cc} K_r & -K_i \\ K_i & K_r \end{array} \right), \bar{\mathbf{h}} = \left(\begin{array}{c} \mathbf{h}_i \\ -\mathbf{h}_r \end{array} \right), \quad (31)$$

where the matrix K and the vector $\mathbf{h}$ are the complex quantities of Eq. (13). The Lagrangian multipliers are $\boldsymbol{\lambda} \in \mathbb{R}^j$ and $\bar{M} = \frac{\partial \mathbf{f}}{\partial \bar{\mathbf{z}}}$ with $\mathbf{f} = (f_1, \ldots, f_j)$ is a real valued $j \times 2n_p$ matrix. Details of the implementation of the constrained TDVP are given in [40]. If no constraint is active, i.e., $j = 0$, then Eq. (31) obviously reduces to the real formulation of Eq. (13).

IV. RESULTS AND DISCUSSION

In this section we present examples for the fictitious time wave packet propagation of the hydrogen atom in external fields. Autocorrelation functions between the initial and time propagated wave packets are computed. Quantum spectra are obtained by the frequency analysis of the autocorrelation function and compared with numerically exact diagonalizations of the Hamiltonian.

It turns out that a sensible choice of an appropriate initial state $\psi(0)$ is crucial for the successful application of the TDVP. For an unreasonable choice the numerical problems discussed in Sec. III C 2 occur for few basis states already, and bad, unconverged results are obtained. The conventional way to construct an initial wave packet by placing a certain number of unrestricted GWPs at various positions in coordinate and momentum space is not possible for the restricted GWPs in the KS coordinates. In the calculations of the diamagnetic and the crossed fields hydrogen atom we achieved optimal results by first choosing only one 2D or 3D Gaussian wave packet in the physical coordinates, which was then expanded in a set of N restricted GWPs as explained in Ref. [30] for the field-free hydrogen atom. The external fields lead to couplings between the basis states and imply a complicated time development of the initial state as compared to the field-free hydrogen atom, where the wave packet propagation is periodic in time [30].

A. Diamagnetic hydrogen atom

The initial wave function is most conveniently chosen to be a GWP in parabolic coordinates

$$\psi(\xi, \eta) = A \exp \left[-(\xi - \xi_0)^2/(4\sigma^2) - (\eta - \eta_0)^2/(4\sigma^2) \right.$$
$$\left. + ip_{\xi_0}(\xi - \xi_0) + ip_{\eta_0}(\eta - \eta_0) \right], \quad (32)$$

with center (ξ_0, η_0), width σ and mean momentum (p_{ξ_0}, p_{η_0}). The GWP is expanded in terms of the basis states (17) according to the procedure described in detail in Ref. [30], including the Monte Carlo technique with importance sampling. The procedure yields the initial values of the variational parameters $\gamma^k, a_\mu^k, a_\nu^k, \ k = 1, \ldots, N$.

However, it is not realistic to propagate several thousands of basis states numerically with the full coupling. Reliable results are obtained by far fewer basis states than used in the expansion and propagation of the GWP (32) in the field-free hydrogen atom [30]. Reasonable numbers of basis states are in the range of N=10-100. A numerical example is presented for the magnetic quantum number $m = 0$, where $N = 70$ basis states are used for the expansion and propagation. The damping factor ϵ is set to $\epsilon = 0.1$

Each basis state has three variational parameters $\gamma^k, a_\mu^k, a_\nu^k$, and therefore N basis states require the solution of a $3N \times 3N$ matrix equation after every integration step, and the usual numerical problems mentioned in Sec. III occur with increasing number of basis states. It turns out that constraints on the imaginary parts of the phase parameters of the form $\text{Im}\gamma^k \geq \gamma_{\min} = -4.5; k = 1, \ldots, N$ are suitable to regularize the equations of motion with regard to a fast integration. These constraints present simple lower bounds on the amplitudes of the wave packets and avoid matrix singularities caused by extremely large overlapping wave packets.

The accuracy of the expansion (32) of the GWP with only $N = 70$ basis states is very good. The time evolution of the wave function is shown in Fig. 2. The probability density $\rho|\psi(\rho, z)|^2$ for six different times $\tau = 0.4, 0.8, 1.2, 3.0, 5.0, 7.0$ is shown. The parameters of the potential in the Hamiltonian (9) are set to $\alpha = 0.5$ and $\beta = 0.2$. The π periodicity of the evolution of the wave function that is present in the field-free hydrogen atom, is destroyed now.

The autocorrelation function of the propagation can be used to extract spectral information by Fourier transformation or harmonic inversion [41–45] of the time signal. The center of the Gaussian (32) is $\rho_0 = 6, z_0 = 0$ and the initial mean momentum is chosen in such a way that states around an effective quantum number of $n_{\text{eff}} \approx 6$ are excited.

To reduce the density of states the autocorrelation function is separately computed for the subspaces of even and odd parity by taking the symmetrized and antisymmetrized states $\psi_0^\pm(\rho, z) = \psi_0(\rho, z) \pm \psi_0(\rho, -z)$. The autocorrelation function $C^\pm(\tau) = \langle \psi_0^\pm(0) | \psi_0^\pm(\tau) \rangle$, is shown in Fig. 3(a) for symmetrized states and in Fig. 3(b) for the antisymmetric states. The spectral results for the diamagnetic hydrogen atom, obtained from the time signals are plotted in Fig. 4. A harmonic inversion has been employed. The amplitudes of the peaks are determined by the magnitude of the overlap between the eigenstates, denoted by $|n_{\text{eff}}\rangle$, and the initial states $\psi_0^\pm(0)$ in Fig. 4(a) and Fig. 4(b), respectively. The amplitudes are plotted with red lines. The numerically exact eigenvalues of the diamagnetic hydrogen atom are plotted with blue lines
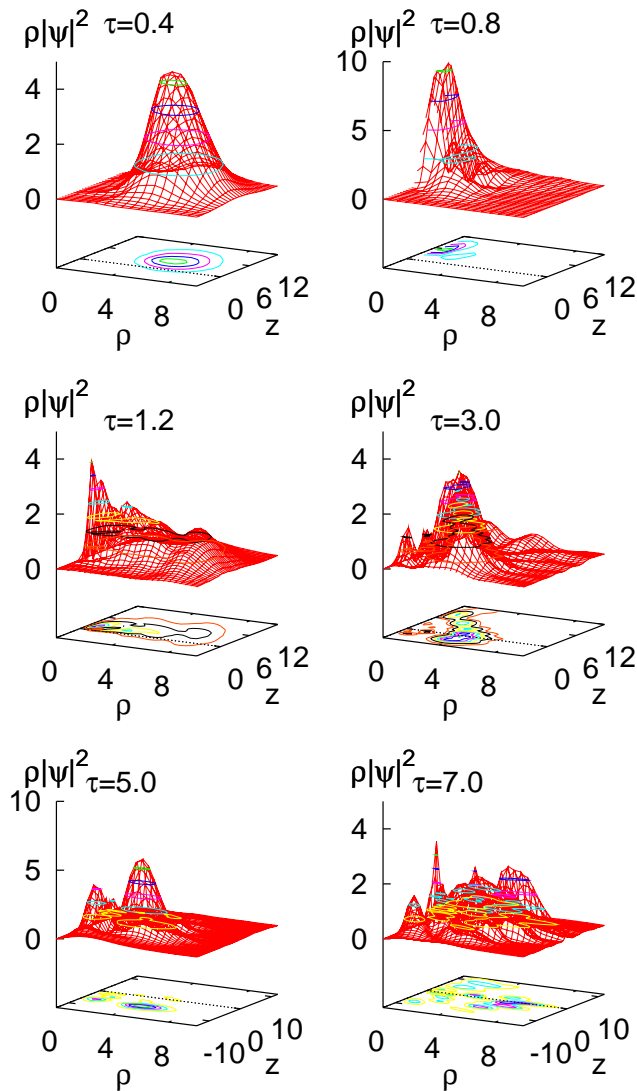
FIG. 2: (Color online) Fictitious time evolution of the state (32) with $\rho_0 = 6.0, z_0 = 0$ and a nonzero initial mean momentum. The wave function is plotted for the times $\tau = 0.4, 0.8, 1.2, 3.0, 5.0, 7.0$. The initial wave packet gradually becomes delocalized.

for comparison. The agreement of the positions is excellent. The highest amplitudes are located in the region $n_{\text{eff}} \approx 6$ according to the choice of the input parameters of the initial GWP in Eq. (32). The multiplicity of the states with even or odd z-parity resulting from the same principle quantum number n is determined by the number of positive and negative eigenvalues $(-1)^{l+m}$ of the z-parity operator acting on the spherical harmonics $Y_{lm}(\theta, \varphi)$ with $l < n$.

The values of the parameters $\alpha = 0.5$ and $\beta = 0.2$ used for this computation still present a mainly harmonic system with a perturbation for low energies. However, the method even allows for the computation of eigenvalues in the strong anharmonic regime. Fig. 5 presents re-
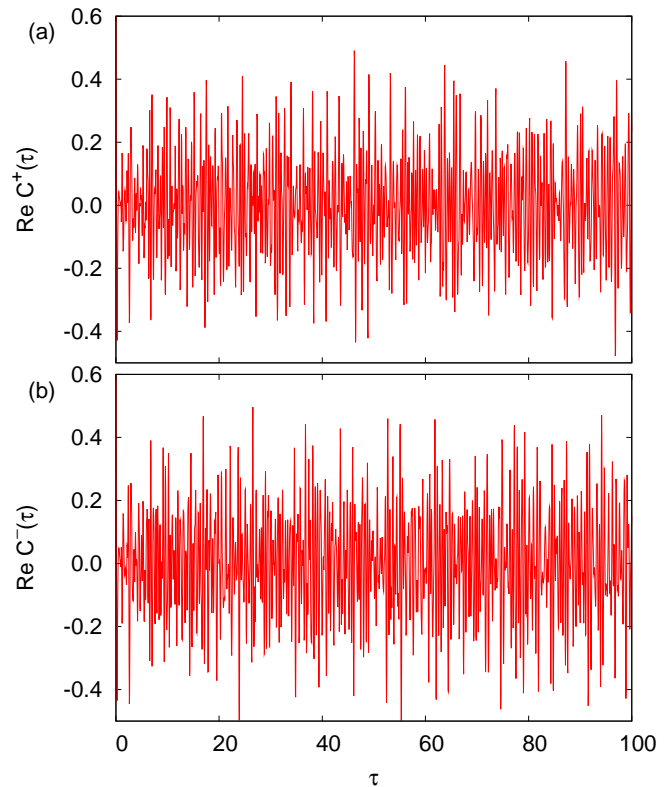

FIG. 3: (Color online) Real part of the autocorrelation function $C^{\pm}(\tau) = \langle \psi_0^{\pm}(0) | \psi_0^{\pm}(\tau) \rangle$ for the GWP (32) with the center $\rho_0 = 6.0, z_0 = 0$. (a) Signal of the projected state with even parity, and (b) odd parity.

sults at the field-free ionization energy $E = \alpha = 0$ and $\beta = 0.5$ for (a) even parity and (b) odd parity. A number of $N = 90$ basis states was used in the computation. In the presence of the magnetic field these states at the field-free ionization energy $E = 0$ are still bound. The agreement between the eigenvalues computed variationally (red lines) and the numerically exact results (blue lines) is very good. The related field strengths are easily obtained from Eq. (4) by $B = \beta/n_{\text{eff}}^2$ The underlying initial wave packet (32) is initially centered at $\rho_0 = 4.39, z_0 = 1$ and has zero mean momentum. Some lines are lacking in the variational computation. The reason is that some amplitudes, i.e., the overlaps of the respective eigenstates $|n_{\text{eff}}\rangle$ and the initial GWP, are nearly zero.

B. Hydrogen atom in crossed fields

Finally, we present example calculations for the hydrogen atom in crossed electric and magnetic fields. The propagation of 3D GWPs is computed for the time-dependent Schrödinger equation (2) with parameters $\alpha = 0.5$, $\beta = 0.05$, and $\zeta = 0.01$ in Eq. (4). The choice of an appropriate initial state $\psi(0)$ is very important for the successful application of the TDVP. We achieved optimal
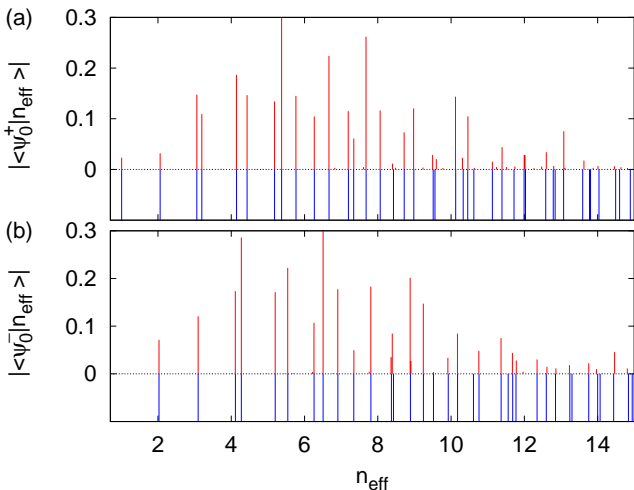
FIG. 4: (Color online) Spectra with (a) even and (b) odd z-parity extracted from the autocorrelation function $C^{\pm}(\tau) = \langle \psi_0^{\pm}(\tau = 0)|\psi_0^{\pm}(\tau)\rangle$ computed from the evolution of the wave function (32) plotted in Fig. 2 ($\tau \geq 0$). The amplitudes are given by the magnitude of overlap between the initial wave function and the respective eigenstates. For comparison the positions of the numerically exact eigenvalues obtained from a diagonalization are plotted with blue lines. The related eigenenergies and the magnetic field strength follow simply from Eq. (4).

results by first choosing one 3D Gaussian wave packet in physical Cartesian coordinates with the center $\mathbf{x}_0$ and width σ in position space and center $\mathbf{p}_0$ in momentum space

$$\psi(\mathbf{x}) = (2\pi\sigma^2)^{-3/4} \exp\left\{-\frac{(\mathbf{x} - \mathbf{x}_0)^2}{4\sigma^2} + i\mathbf{p}_0 \cdot (\mathbf{x} - \mathbf{x}_0)\right\} \tag{33}$$

which is then expanded in a set of N restricted GWPs. The external fields lead to couplings between the basis states, and the time-dependence of the variational parameters must be determined by the numerical integration of Eq. (25). For better numerical performance we resort to the TDVP with constraints [40] mentioned in Sec. III C 2. As for the diamagnetic hydrogen atom constraints of the form $\gamma_{\min} = -4.0 \leq \mathrm{Im}\gamma^k$, $k = 1, \ldots, N$ are imposed on the imaginary parts of the phase parameters γ^k. Once a time-dependent wave packet (6) is determined the eigenvalues n_{eff} of the stationary Schrödinger equation (2) are obtained by the frequency analysis of the time signal (10) with the amplitudes c_j depending on the choice of the initial wave packet. In perpendicular crossed fields the z parity is conserved. Spectra with even and odd z parity obtained from the Fourier transforms of the autocorrelation functions $C^{\pm}(\tau) = \langle \psi^{\pm}(0)|\psi^{\pm}(\tau)\rangle$ of the parity projected wave packets are shown in Fig. 6. In Fig. 6(a) the eigenvalues with even parity and in Fig. 6(b) the eigenvalues with odd parity are plotted. The green and red lines result from the propagation of two different 3D GWPs with $\sigma = 3.5$, $\epsilon = 0.15$ and the
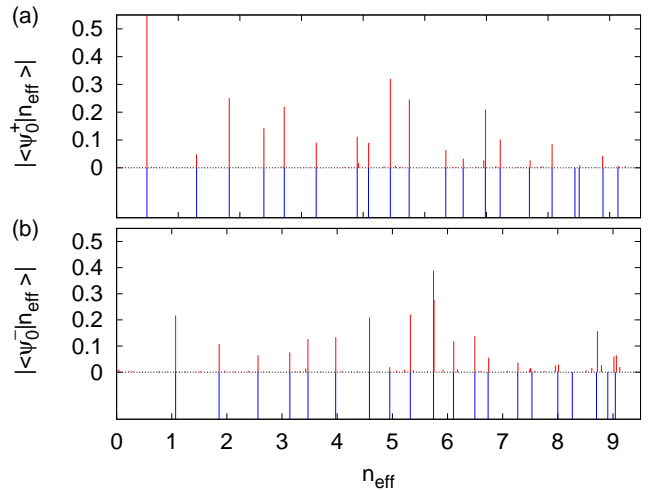

FIG. 5: (Color online) Effective quantum numbers n_{eff} at the field-free ionization threshold $E = \alpha = 0$ for states of (a) even and (b) odd parity. The propagation involves $N = 90$ basis states. The variational results (red lines) are in excellent agreement with the exact time-independent results (blue lines).

same initial position $\mathbf{x}_0 = (6, 0, 0)$ but different initial mean momenta $\mathbf{p}_0 = (0, \pm 1/\sqrt{2}, 1/\sqrt{2})$, respectively. A number of $N = 41$ and $N = 31$ basis states were coupled in the calculations. The line widths, i.e., the resolution of the spectra, is determined by the length of the time signal $\tau_{\max}$. The eigenvalues obtained by numerically exact diagonalizations of the stationary Hamiltonian (2) are shown by the blue lines. The line-by-line comparison shows good agreement between the exact spectrum and the results obtained by the wave packet propagation. The amplitudes of levels indicate the excitation strengths of states with higher or lower angular momentum l_z by the two initial wave packets rotating clockwise or anticlockwise around the z axis.

V. CONCLUSION

The Gaussian wave packet method is known to be well suited for systems with nonsingular smooth potentials but not so for systems with singular potentials such as the Coulomb potential. Therefore so far it failed when applied to atomic systems. Using the Kustaanheimo-Stiefel regularization of the Coulomb potential and introducing a fictitious time variable we have now made it applicable to atomic systems by using restricted GWPS and the time-dependent variational principle. The special appeal of the GWP method lies in the fact that relatively low numbers of time-dependent basis states are sufficient to derive the spectrum as compared to time-independent matrix diagonalizations. The advantage of using the fictitious time is that the computations are exact and analytical for the field-free hydrogen atom, which means that
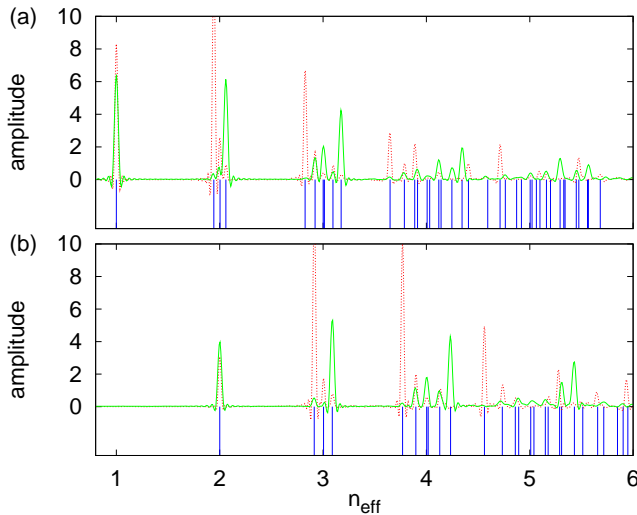
FIG. 6: (Color online) Spectra with (a) even and (b) odd z parity of the Hamiltonian (2) with $\alpha = 0.5$, $\beta = 0.05$, $\zeta = 0.01$ obtained from the propagation of two different 3D GWPs. Green and red line: $\mathbf{x}_0 = (6, 0, 0)$, $\mathbf{p}_0 = (0, \pm 1/\sqrt{2}, 1/\sqrt{2})$, respectively. The eigenvalues are extracted from the autocorrelation function by Fourier transformation. The peak positions agree very well with the numerically exact eigenvalues of the effective quantum number marked by blue lines. The related eigenenergies and the field strengths follow from Eq. (4).

for perturbed atomic systems only the deviation of the potential from the Coulomb part must be taken into account in the variational approximation. We have shown that the method can be especially adapted for systems with, e.g., cylindrical or spherical symmetries and thus allows for a wide range of future applications.

Appendix A: Integrals for the diamagnetic hydrogen atom

With the basis functions g_m defined in Eq. (17), and using the notation $a_\mu \equiv a_\mu^k - (a_\mu^l)^*$, $a_\nu \equiv a_\nu^k - (a_\nu^l)^*$, $\gamma \equiv \gamma^k - (\gamma^l)^*$, and $m \geq 0$, the absolute value of the magnetic quantum number the integrals in Eq. (20) take the form

$$\langle g_m^l | f(\mu, \nu) | g_m^k \rangle$$
$$= 4\pi^2 \int_0^\infty d\mu \int_0^\infty d\nu (\mu\nu)^{2m+1} f(\mu^2, \nu^2) e^{i(a_\mu \mu^2 + a_\nu \nu^2 + \gamma)} , \tag{A1}$$

where $f(\mu^2, \nu^2)$ is a poynomial in μ^2 and ν^2. The integrals can be factorized, and with $x = \mu^2$ or $x = \nu^2$ the products basically take the elementary form $\int_0^\infty x^n e^{-ax} dx = \frac{n!}{a^{n+1}}$ for integers $n \geq 0$ and $\operatorname{Re} a > 0$. The integrals on the left-hand side of Eq. (20) read

$$
\begin{aligned}
\langle g_m^l | g_m^k \rangle &= \frac{\pi^2 (m!)^2}{(-a_\mu a_\nu)^{m+1}} e^{i\gamma} \equiv c , \\
\langle g_m^l | \mu^2 | g_m^k \rangle &= \frac{c}{-i a_\mu}(m+1) , \\
\langle g_m^l | \nu^2 | g_m^k \rangle &= \frac{c}{-i a_\nu}(m+1) , \\
\langle g_m^l | \mu^4 | g_m^k \rangle &= \frac{c}{-a_\mu^2}(m+1)(m+2) , \\
\langle g_m^l | \mu^2 \nu^2 | g_m^k \rangle &= \frac{c}{-a_\mu a_\nu}(m+1)^2 , \\
\langle g_m^l | \nu^4 | g_m^k \rangle &= \frac{c}{-a_\nu^2}(m+1)(m+2) .
\end{aligned}
\tag{A2}
$$

With the potential $V(\mu, \nu)$ given in Eq. (9) the integrals on the right-hand side of Eq. (20) are obtained as

$$
\begin{aligned}
\langle g_m^l | V(\mu, \nu) | g_m^k \rangle &= \frac{-ic}{8 a_\mu^2 a_\nu^2}(a_\mu + a_\nu)(1+m)[(2+3m+m^2)\beta^2 + 8 a_\mu a_\nu \alpha] , \\
\langle g_m^l | \mu^2 V(\mu, \nu) | g_m^k \rangle &= \frac{c}{8 a_\mu^3 a_\nu^2}(m+1)\{(1+m)(2+m)[a_\mu(2+m) + a_\nu(3+m)]\beta^2 + 8 a_\mu a_\nu[a_\mu + 2a_\nu + (a_\mu + a_\nu)m]\alpha\} , \\
\langle g_m^l | \nu^2 V(\mu, \nu) | g_m^k \rangle &= \frac{c}{8 a_\mu^2 a_\nu^3}(m+1)\{(1+m)(2+m)[a_\mu(3+m) + a_\nu(2+m)]\beta^2 + 8 a_\mu a_\nu[2a_\mu + a_\nu + (a_\mu + a_\nu)m]\alpha\} .
\end{aligned}
$$

Appendix B: Integrals for the hydrogen atom in crossed fields

The integrals in the linear set of equations (27) take the form

$$\langle g^l | f(\mathbf{u}, \nabla_{\mathbf{u}}) | g^k \rangle$$
$$= \int d^4 u\, e^{-i[\mathbf{u}(A^l)^*\mathbf{u} + (\gamma^l)^*]} f(\mathbf{u}, \nabla_{\mathbf{u}}) e^{i[\mathbf{u}A^k\mathbf{u} + \gamma^k]} . \tag{B1}$$

With the notation $A = A^k - (A^l)^*$, $\gamma = \gamma^k - (\gamma^l)^*$ the integrals on the left-hand side of Eq. (27) simplify to

$$I_{ij}^{lk} = \langle g^l | f_i f_j | g^k \rangle = \int d^4 u\, f_i f_j e^{i(\mathbf{u}A\mathbf{u} + \gamma)} , \tag{B2}$$

with $f_1 = 1$, $f_2 = u_1^2 + u_2^2$, $f_3 = u_3^2 + u_4^2$, $f_4 = u_1 u_3 - u_2 u_4$, and $f_5 = u_1 u_4 + u_2 u_3$. The integrals have the properties $I_{ij}^{lk} = (I_{ij}^{kl})^*$ and $I_{ij}^{lk} = I_{ji}^{lk}$. Using $c = \pi^2 e^{i\gamma}$ and $h = 1/\sqrt{-\det A} = 1/(a_x^2 + a_y^2 - a_\mu a_\nu)$ we obtain

$$I_{11}^{lk} = hc \ , \ I_{12}^{lk} = -ia_\nu h^2 c \ , \ I_{13}^{lk} = -ia_\mu h^2 c \ ,$$
$$I_{14}^{lk} = 2ia_x h^2 c \ , \ I_{15}^{lk} = 2ia_y h^2 c \ , \ I_{22}^{lk} = -2a_\nu^2 h^3 c \ ,$$
$$I_{23}^{lk} = -(a_\mu a_\nu + a_x^2 + a_y^2)h^3 c \ , \ I_{24}^{lk} = 4a_\nu a_x h^3 c \ ,$$
$$I_{25}^{lk} = 4a_\nu a_y h^3 c \ , \ I_{33}^{lk} = -2a_\mu^2 h^3 c \ , \ I_{34}^{lk} = 4a_\mu a_x h^3 c \ ,$$
$$I_{35}^{lk} = 4a_\mu a_y h^3 c \ , \ I_{44}^{lk} = 2(a_y^2 - 3a_x^2 - a_\mu a_\nu)h^3 c \ ,$$
$$I_{45}^{lk} = -8a_x a_y h^3 c \ , \ I_{55}^{lk} = 2(a_x^2 - 3a_y^2 - a_\mu a_\nu)h^3 c \ . \quad (B3)$$

The integrals on the right-hand side of Eq. (27) are defined as

$$I_{vj}^{lk} = \langle g^l | f_j V | g^k \rangle \ . \quad (B4)$$

The potential V defined via Eq. (2) can be split into its harmonic and diamagnetic part,

$$V_a = \alpha \mathbf{u}^2 + \frac{1}{8}\beta^2 (u_1^2 + u_2^2)(u_3^2 + u_4^2)\mathbf{u}^2 \ , \quad (B5)$$

and the terms of the paramagnetic and electric field contributions,

$$V_b = \frac{1}{2}\beta \left[(u_1 p_2 - u_2 p_1)(u_3^2 + u_4^2) \right. \quad (B6)$$
$$\left. + (u_3 p_4 - u_4 p_3)(u_1^2 + u_2^2) \right] + \zeta(u_1 u_3 - u_2 u_4)\mathbf{u}^2 \ .$$

Note that the paramagnetic term in Eq. (B7) contains derivatives with respect to the KS coordinates and thus the integrals must be solved by application of Eq. (B1). We obtain

$$I_{v1a}^{lk} = i(a_\mu + a_\nu)[(a_\mu a_\nu + 2(a_x^2 + a_y^2))\beta^2 h^2/4 + \alpha]h^2 c \ ,$$
$$I_{v2a}^{lk} = [2a_\mu^2 a_\nu^2 + (a_x^2 + a_y^2)(9a_\nu^2 + 2(a_x^2 + a_y^2)) + a_\mu a_\nu(3a_\nu^2 + 8(a_x^2 + a_y^2))]\beta^2 h^5 c/4 + [a_\nu(a_\mu + 2a_\nu) + a_x^2 + a_y^2]\alpha h^3 c \ ,$$
$$I_{v3a}^{lk} = [3a_\mu^3 a_\nu + 8a_\mu a_\nu(a_x^2 + a_y^2) + 2(a_x^2 + a_y^2)^2 + a_\mu^2(2a_\nu^2 + 9(a_x^2 + a_y^2))]\beta^2 h^5 c/4 + [a_\mu(2a_\mu + a_\nu) + a_x^2 + a_y^2]\alpha h^3 c \ ,$$
$$I_{v4a}^{lk} = -(a_\mu + a_\nu)a_x[3(a_\mu a_\nu + a_x^2 + a_y^2)\beta^2 h^2 + 4\alpha]h^3 c \ ,$$
$$I_{v5a}^{lk} = -(a_\mu + a_\nu)a_y[3(a_\mu a_\nu + a_x^2 + a_y^2)\beta^2 h^2 + 4\alpha]h^3 c \ , \quad (B7)$$

$$I_{v1b}^{lk} = 2(a_\mu + a_\nu)(a_y^k a_x \beta - a_x^k a_y \beta + a_x \zeta)h^3 c \ ,$$
$$I_{v2b}^{lk} = -2i(2a_\mu a_\nu + 3a_\nu^2 + a_x^2 + a_y^2)(a_y^k a_x \beta - a_x^k a_y \beta + a_x \zeta)h^4 c \ ,$$
$$I_{v3b}^{lk} = -2i(3a_\mu^2 + 2a_\mu a_\nu + a_x^2 + a_y^2)(a_y^k a_x \beta - a_x^k a_y \beta + a_x \zeta)h^4 c \ ,$$
$$I_{v4b}^{lk} = 2i(a_\mu + a_\nu)[-6a_x^k a_x a_y \beta + a_y^k(a_\mu a_\nu + 5a_x^2 - a_y^2)\beta + (a_\mu a_\nu + 5a_x^2 - a_y^2)\zeta]h^4 c \ ,$$
$$I_{v5b}^{lk} = -2i(a_\mu + a_\nu)[a_x^k(a_\mu a_\nu - a_x^2 + 5a_y^2)\beta - 6a_x a_y(a_y^k \beta + \zeta)]h^4 c \ , \quad (B8)$$

where a_x^k and a_y^k are elements of the width matrix A^k. The right-hand side vector in Eq. (27) is the sum of two corresponding terms in Eqs. (B7) and (B8), i.e., $I_{vj}^{lk} = I_{vja}^{lk} + I_{vjb}^{lk}$ for $j = 1, \ldots, 5$.

Appendix C: Structure of the matrices B and C

A structure of the matrices B^k and C^k is searched which is preserved in the matrix product $V_2^k C^k$ in Eq. (29), where V_2^k has the same structure as A in Eq. (7). This is provided by the form

$$B = \begin{pmatrix} b_{11} & b_{12} & b_{13} & b_{14} \\ -b_{12} & b_{11} & b_{14} & -b_{13} \\ b_{31} & b_{32} & b_{33} & b_{34} \\ b_{32} & -b_{31} & -b_{34} & b_{33} \end{pmatrix} \ ,$$

$$C = \begin{pmatrix} c_{11} & c_{12} & c_{13} & c_{14} \\ -c_{12} & c_{11} & c_{14} & -c_{13} \\ c_{31} & c_{32} & c_{33} & c_{34} \\ c_{32} & -c_{31} & -c_{34} & c_{33} \end{pmatrix} \ , \quad (C1)$$

as can easily be shown by explicit multiplication. The superscript k running over all GWPs has been omitted here. Compared to Eq. (7) the number of independent parameters per matrix increases from 4 to 8, however, this is still less than 16 parameters for a general 4×4 matrix without any special structure.

The matrix $A = \frac{1}{2}BC^{-1}$ can be calculated analytically. To this end we introduce the auxiliary matrix

$$D = \begin{pmatrix} c_{33} & -c_{34} & -c_{13} & -c_{14} \\ c_{34} & c_{33} & -c_{14} & c_{13} \\ -c_{31} & -c_{32} & c_{11} & -c_{12} \\ -c_{32} & c_{31} & c_{12} & c_{11} \end{pmatrix} \ . \quad (C2)$$

The product $C_1 = CD$ yields

$$C_1 = \begin{pmatrix} h & k & 0 & 0 \\ -k & h & 0 & 0 \\ 0 & 0 & h & -k \\ 0 & 0 & k & h \end{pmatrix}, \qquad (C3)$$

with $\begin{cases} h = -c_{13}c_{31} - c_{14}c_{32} + c_{11}c_{33} + c_{12}c_{34}\,, \\ k = c_{14}c_{31} - c_{13}c_{32} + c_{12}c_{33} - c_{11}c_{34}\,. \end{cases}$

The matrix C_1 can be easily inverted, and thus allows for the calculation of $A = \frac{1}{2}BC^{-1} = \frac{1}{2}BDC_1^{-1}$. With $h' \equiv h/[2(h^2 + k^2)]$, $k' \equiv k/[2(h^2 + k^2)]$ the four independent parameters in Eq. (7) read

$$\begin{aligned} a_\mu &= (b_{11}c_{33} - b_{14}c_{32} + b_{12}c_{34} - b_{13}c_{31})h' \\ &\quad + (b_{14}c_{31} + b_{12}c_{33} - b_{11}c_{34} - b_{13}c_{32})k'\,, \\ a_\nu &= (b_{33}c_{11} + b_{34}c_{12} - b_{31}c_{13} - b_{32}c_{14})h' \\ &\quad + (b_{33}c_{12} - b_{34}c_{11} - b_{32}c_{13} + b_{31}c_{14})k'\,, \\ a_x &= (b_{13}c_{11} + b_{14}c_{12} - b_{11}c_{13} - b_{12}c_{14})h' \\ &\quad + (b_{13}c_{12} - b_{14}c_{11} - b_{12}c_{13} + b_{11}c_{14})k'\,, \\ a_y &= (b_{14}c_{11} - b_{13}c_{12} + b_{12}c_{13} - b_{11}c_{14})h' \\ &\quad + (b_{13}c_{11} + b_{14}c_{12} - b_{11}c_{13} - b_{12}c_{14})k'\,. \quad (C4) \end{aligned}$$

[1] A. Holle, J. Main, G. Wiebusch, H. Rottke, and K. H. Welge, Phys. Rev. Lett. **61**, 161 (1988).
[2] H. Friedrich and D. Wintgen, Phys. Rep. **183**, 37 (1989).
[3] H. Hasegawa, M. Robnik, and G. Wunner, Prog. Theor. Phys. Suppl. **98**, 198 (1989).
[4] J. Main, G. Wiebusch, K. H. Welge, J. Shaw, and J. B. Delos, Phys. Rev. A **49**, 847 (1994).
[5] T. Fabčič, J. Main, T. Bartsch, and G. Wunner, J. Phys. B **38**, S219 (2005).
[6] G. Wiebusch, J. Main, K. Krüger, H. Rottke, A. Holle, and K. H. Welge, Phys. Rev. Lett. **62**, 2821 (1989).
[7] J. Main and G. Wunner, Phys. Rev. Lett. **69**, 586 (1992).
[8] J. Main and G. Wunner, J. Phys. B **27**, 2835 (1994).
[9] J. v. Milczewski, G. H. F. Diercksen, and T. Uzer, Phys. Rev. Lett. **76**, 2890 (1996).
[10] C. Neumann, R. Ubert, S. Freund, E. Flöthmann, B. Sheehy, K. H. Welge, M. R. Haggerty, and J. B. Delos, Phys. Rev. Lett. **78**, 4705 (1997).
[11] S. Freund, R. Ubert, E. Flöthmann, K. H. Welge, D. M. Wang, and J. B. Delos, Phys. Rev. A **65**, 053408 (2002).
[12] T. Bartsch, J. Main, and G. Wunner, Phys. Rev. A **67**, 063410 (2003).
[13] T. Bartsch, J. Main, and G. Wunner, Phys. Rev. A **67**, 063411 (2003).
[14] S. Gekle, J. Main, T. Bartsch, and T. Uzer, Phys. Rev. Lett. **97**, 104101 (2006).
[15] S. Gekle, J. Main, T. Bartsch, and T. Uzer, Phys. Rev. A **75**, 023406 (2007).
[16] H. Cartarius, J. Main, and G. Wunner, Phys. Rev. Lett. **99**, 173003 (2007).
[17] M. L. Du and J. B. Delos, Phys. Rev. A **38**, 1896 and 1913 (1988).
[18] E. B. Bogomolny, Sov. Phys. JETP **69**, 275 (1989).
[19] M. C. Gutzwiller, *Chaos in Classical and Quantum Mechanics* (Springer, New York, 1990).
[20] M. Brack and R. K. Bhaduri, *Semiclassical Physics*, vol. 96 of *Frontiers in Physics* (Addison-Wesley Publishing Company, Reading, Mass., 1997).
[21] G. Tanner, K. T. Hansen, and J. Main, Nonlinearity **9**, 1641 (1996).
[22] A. D. McLachlan, Mol. Phys. **8**, 39 (1964).
[23] E. J. Heller, J. Chem. Phys. **62**, 1544 (1975).
[24] E. J. Heller, J. Chem. Phys. **64**, 63 (1976).
[25] I. M. S. Barnes, M. Nauenberg, M. Nockleby, and S. Tomsovic, Phys. Rev. Lett. **71**, 1961 (1993).
[26] I. M. S. Barnes, M. Nauenberg, M. Nockleby, and S. Tomsovic, J. Phys. A **27**, 3299 (1994).
[27] I. M. S. Barnes, Chaos, Solitons & Fractals **6**, 531 (1995).
[28] A. Buchleitner and D. Delande, Phys. Rev. Lett. **75**, 1487 (1995).
[29] C. Cerjan, E. Lee, D. Farrelly, and T. Uzer, Phys. Rev. A **55**, 2222 (1997).
[30] T. Fabčič and J. Main, preceding paper, preprint.
[31] S.-I. Sawada, R. Heather, B. Jackson, and H. Metiu, J. Chem. Phys. **83**, 3009 (1985).
[32] W. H. Press, S. A. Teukolsky, W. T. Vetterling, and B. P. Flannery, *Numerical Recipes* (University Press, Cambridge, 1992).
[33] E. J. Heller, J. Chem. Phys. **65**, 4979 (1976).
[34] F. Hansen, N. E. Henriksen, and G. D. Billing, J. Chem. Phys. **90**, 3060 (1989).
[35] K. G. Kay, Chem. Phys. **137**, 165 (1989).
[36] R. Heather and H. Metiu, J. Chem. Phys. **84**, 3250 (1986).
[37] I. Horenko, M. Weiser, B. Schmidt, and C. Schütte, J. Chem. Phys. **120**, 8913 (2004).
[38] R. T. Skodje and D. G. Truhlar, J. Chem. Phys. **80**, 3123 (1984).
[39] J. Zoppe, M. L. Parkinson, and M. Messina, Chem. Phys. Lett. **407**, 308 (2005).
[40] T. Fabčič, J. Main, and G. Wunner, J. Chem. Phys. **128**, 044116 (2008).
[41] M. R. Wall and D. Neuhauser, J. Chem. Phys. **102**, 8011 (1995).
[42] V. A. Mandelshtam and H. S. Taylor, J. Chem. Phys **107**, 6756 (1997).
[43] J. Main, Phys. Rep. **316**, 233 (1999).
[44] J. Main, P. A. Dando, Dž. Belkic, and H. S. Taylor, J. Phys. A **33**, 1247 (2000).
[45] Dž. Belkić, P. A. Dando, J. Main, and H. S. Taylor, J. Chem. Phys. **113**, 6542 (2000).